Intelligent Optimal Feed-Back Torque Control of a 6DOF Surgical Rotary Robot

Farzam Tajdari
School of Enginnering
Delf University of Technology
Delft, Netherlands
f.tajdari@tudelft.nl

Naeim Ebrahimi Toulkani
Aerospace Enginnering
Sharif University of Technology
Tehran, Iran
naeim.ebrahimi@alum.sharif.edu

Nima Zhilakzadeh
Mechanical Engineering
I.K.I University
Qazvin, Iran
Nimazhilak@gmail.com

***Abstract*— Surgical robotic revolution has assisted surgeons to perform sophisticated surgeries, and increased accuracy, reduced risk, operative and recovery time. Parallel mechanisms are widely used for designing of surgical robots due to their advantage of low inertia and high precision. Specific surgical procedures confine, and restrict their workspace, while controlling and validating the robots are complicated regarding to their complex dynamic. To this end, in this paper, a 6-DOF robot, with rotary manipulators, is designed and controlled. Addressing nonlinearity of parallel robots, a novel approach is designed to robustly penalize the error of tracking at end effector employing a Linear Quadratic Integral (LQI) regulator with online Artificial Neural Network (ANN) gain tuning, based on non-linear model in format of a Linear Time Invariant (LTI) model. As validation, the controller is implemented using MATLAB on the non-linear model designed in Adams software online. Simulation results demonstrates the optimal controller penalizing the error while minimizing torque on each rotary manipulator. In addition, the method defines the workspace of both the states and torques, which is an introduction to comprehensive design of such robots.**

Keywords*— *parallel rotary robot, validation, optimal control, nonlinear systems.

I. INTRODUCTION

Nowadays, surgical robots play significant role in medical science and the usage of them is growing every year. Regarding to innovation created in surgical robots' hardware and software, automation in the field has witnessed considerable improvements.

Static training cadres for surgeries are studied in [1]. Furthermore, the Fundamentals of Laparoscopic Surgery (FLS) [2] and the Fundamental Skills of Robotic Surgery (FSRS) [3] can be mentioned as some developments that have been facilitated by medical society. Also, these cadres identify some useful duties that simulate key surgical techniques in static status. In spite of the advantages, mentioned methods are not able to simulate humans' body actions such as breathing, heartbeat etc. which exist in most of the surgeries [4, 5].

For evaluating automation, needs dynamic motion and a software interface for inverse kinematics and internal state-estimation, a low-cost platform (total cost less than $250) named miniaturized Stewart platform [6, 7] has been designed and used.

There are some recent studies about dynamics of the Stewart robot. Simplified dynamic models, by neglecting the effects of the legs and friction, were proposed in [8, 9], and was improved considering a simplified model for the legs in [10, 11]. In [12] a comprehensive model is developed based on the Newton–Euler approach considering the viscous friction for the joints. Lagrange method was used in [13]. Various other methods were also proposed, such as the recursive matrix method [14], Kane's equations [15, 16], principle of virtual work [17], generalized momentum approach [18], and screw theory [19].

Most of approaches for Stewart position control in task-space are dependent on dynamic model. Reliable PID controllers are developed only for regulation, unless the position control strategy is employed in the joint space [20]. Although, control schemes of the inverse dynamic model are, in principle, effective for manipulator position control, actuators saturation may be raised [21]. Meanwhile, there are not many studies investigate torque control of a rotary Stewart robot. Recently, several methods introduced to force control of robots, including stiffness control, impedance control, admittance control, hybrid control, explicit force control and implicit force control [22], [23], [24], [25]. While validation of the methods in a reliable non-linear model were missed, and probably causes unsuccessful implementation. Due to mismatch between simulated model and real environment. Moreover, parallel mechanisms and optimization are always involved regarding to redundancy of parallel robots. Thus, this paper aims to, not only design an optimal controller for the complicated parallel mechanism to minimize the torques, but also, validate the controller on a reliable non-linear system, through Adams software.

Paper is organized as follow: Dynamic equation of Stewart robot is presented in II, while controller design is laid in section III. Simulation setup and results, and conclusion are presented in section IV, and V respectively.

II. DYNAMIC EQUATION OF STEWART PLATFORM

To derive the equation of motion, Kinematics and kinetics analysis of robot dynamic are needed. Accordingly, we need to find the relationships between position and velocity of each state prior to dynamic analysis.

A. Kinematics equation

Considering the dynamic of rotary Stewart robot, controllable variables are torques and motor angels (θ_M) manipulated with rotary actuators. Thus, it's worth to find the relationships between controllable variables of motors and end effector discussed as follow:

$$\overline{X} = \begin{bmatrix} \varphi \\ \theta \\ \psi \\ X \\ Y \\ Z \end{bmatrix}, \overline{L} = \begin{bmatrix} L_1 \\ L_2 \\ L_3 \\ L_4 \\ L_5 \\ L_6 \end{bmatrix} = f(\overline{X}), \overline{\theta} = \begin{bmatrix} \theta_1 \\ \theta_2 \\ \theta_3 \\ \theta_4 \\ \theta_5 \\ \theta_6 \end{bmatrix} = g(\overline{L}) \qquad (1)$$

XXX-X-XXXX-XXXX-X/XX/$XX.00 ©20XX IEEE

where, $\overline{X}$ is the end effector's variables, $\overline{L}$ is the distance from joints on base ($\vec{P}_i$) to corresponded joints on end effector ($\vec{p}_i$), and $\overline{\theta}$ is the motor angular shown in Fig. 1. Thus, the relations can be summarized as $\overline{\theta} = g(f(\overline{X}))$. Furthermore, the vector from ($\vec{P}_i$) to ($\vec{p}_i$) can be written as,

$$\vec{L}_i = ({R_{xyz}}^{-1}\vec{p}_i + G) - \vec{P}_i = f(\overline{X}) \quad (2)$$

Where,

$$R_{xyz} = R_x(\varphi)R_y(\theta)R_z(\psi) = \begin{bmatrix} c\theta c\psi & c\theta s\psi & -s\theta \\ c\psi s\theta s\varphi - c\varphi s\psi & c\varphi c\psi + s\theta s\varphi s\psi & c\theta s\varphi \\ c\theta c\psi s\theta + s\varphi s\psi & c\varphi s\theta s\psi - c\psi s\varphi & c\theta c\varphi \end{bmatrix} \quad (3)$$

and,

$$G = \begin{bmatrix} X \\ Y \\ Z \end{bmatrix} \quad (4)$$

Considering, $C\theta_x = Cos(\theta_x), S\theta_x = Sin(\theta_x)$. If we just consider the length of each legs then,

$$\left|\vec{l}_i\right| = \left|{R_{xyz}}^{-1}(\vec{p}_i + G) - (\vec{P}_i + \vec{a}_i)\right| \quad (5)$$

$$\theta_M = -(asind\left(\frac{C}{\sqrt{A^2+B^2}}\right) - acosd\left(\frac{B}{\sqrt{A^2+B^2}}\right) + 180) \quad (6)$$

where $A, B, C \in U(\overline{X})$;

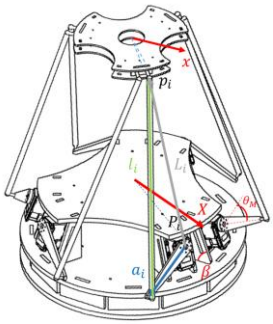

Fig. 1. Free body diagram of a Kinetics equation.

B. Kinetics equation

In this section, dynamic equations of Stewart mechanism are derived using Newton-Euler method. The derivations are summarized just to show different dynamic features of the systems, and the effects. Stewart mechanism, studied in this paper is depicted in Fig. 1 That consist of an end effector, a fixed platform as base, and six legs connected to motors' legs, as manipulators to move the end effector. The legs are connected both from end effector to base platform by spherical joints. Thus, the dynamic equations for end effector can be written as:

$$\sum \vec{M} = \bar{I}\vec{\alpha} \quad (7)$$

$$\sum \vec{F} = \bar{m}\vec{a} \quad (8)$$

$$\begin{bmatrix} \bar{I} & 0_{3\times3} \\ 0_{3\times3} & \bar{m} \end{bmatrix} \begin{bmatrix} \ddot{\varphi} \\ \ddot{\theta} \\ \ddot{\psi} \\ \ddot{X} \\ \ddot{Y} \\ \ddot{Z} \end{bmatrix} = \begin{bmatrix} M \\ F \end{bmatrix} \quad (9)$$

where,

$$\bar{I} = \begin{bmatrix} I_{xx} & 0 & 0 \\ 0 & I_{yy} & 0 \\ 0 & 0 & I_{zz} \end{bmatrix}, \bar{m} = \begin{bmatrix} m & 0 & 0 \\ 0 & m & 0 \\ 0 & 0 & m \end{bmatrix}$$

and,

$$M = \begin{bmatrix} M_x \\ M_y \\ M_z \end{bmatrix}, F = \begin{bmatrix} F_x \\ F_y \\ F_z \end{bmatrix}$$

M and F consist torques and forces exerted on end effector respectively, as shown in Fig. 2. As rotary motors manipulate torques, we need to have the equation in following format.

$$\begin{bmatrix} \bar{I} & 0_{3\times3} \\ 0_{3\times3} & \bar{m} \end{bmatrix} \begin{bmatrix} \ddot{\varphi} \\ \ddot{\theta} \\ \ddot{\psi} \\ \ddot{X} \\ \ddot{Y} \\ \ddot{Z} \end{bmatrix} = \begin{bmatrix} M \\ F \end{bmatrix} = \tau_{6\times6} \begin{bmatrix} T_1 \\ T_2 \\ T_3 \\ T_4 \\ T_5 \\ T_6 \end{bmatrix} \quad (10)$$

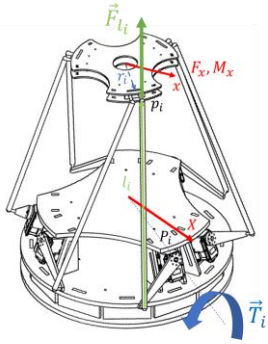

Fig. 2. Dynamic force-torque diagram.

Where T_i is torque produced by motor i. Considering the equation based on their unit vector

$$\sum \vec{M} = \sum \vec{r}_i \times \vec{F}_{l_i} = \sum \vec{p}_i \times \vec{e}_{l_i}\left|\vec{F}_{l_i}\right| = \sum \vec{e}_{M_i}\left|\vec{F}_{l_i}\right| \quad (11)$$

$$\sum \vec{F} = \sum \vec{e}_{l_i}\left|\vec{F}_{l_i}\right| \quad (12)$$

$$\begin{bmatrix} M \\ F \end{bmatrix} = \begin{bmatrix} e_{M_1} & \cdots & e_{M_6} \\ e_{l_1} & \cdots & e_{l_6} \end{bmatrix} \begin{bmatrix} F_{l_1} \\ \vdots \\ F_{l_6} \end{bmatrix} \quad (13)$$

where,

$$\tau_1 = \begin{bmatrix} e_{M_1} & \cdots & e_{M_6} \\ e_{l_1} & \cdots & e_{l_6} \end{bmatrix} \quad (14)$$

As $\vec{F}_{l_i} = \vec{e}_{l_i}.\vec{e}_{N_i}\frac{|\vec{T}_i|}{|\vec{a}_i|}$ then,

$$\begin{bmatrix} F_{l_1} \\ \vdots \\ F_{l_6} \end{bmatrix} = \begin{bmatrix} \frac{\vec{e}_{l_1}.\vec{e}_{N_1}}{|\vec{a}_1|} & \cdots & 0 \\ \vdots & \ddots & \vdots \\ 0 & \cdots & \frac{\vec{e}_{l_6}.\vec{e}_{N_6}}{|\vec{a}_6|} \end{bmatrix} \begin{bmatrix} T_1 \\ \vdots \\ T_6 \end{bmatrix} \quad (15)$$

Considering,

$$\tau_2 = \begin{bmatrix} \frac{\vec{e}_{l_1}.\vec{e}_{N_1}}{|\vec{a}_1|} & \cdots & 0 \\ \vdots & \ddots & \vdots \\ 0 & \cdots & \frac{\vec{e}_{l_6}.\vec{e}_{N_6}}{|\vec{a}_6|} \end{bmatrix} \quad (16)$$

$$\begin{bmatrix} \bar{I} & 0_{3\times3} \\ 0_{3\times3} & \bar{m} \end{bmatrix} \begin{bmatrix} \ddot{\varphi} \\ \ddot{\theta} \\ \ddot{\psi} \\ \ddot{X} \\ \ddot{Y} \\ \ddot{Z} \end{bmatrix} = \begin{bmatrix} M \\ F \end{bmatrix} = \tau_{6\times6} \begin{bmatrix} T_1 \\ T_2 \\ T_3 \\ T_4 \\ T_5 \\ T_6 \end{bmatrix} = \tau_1\tau_2 \begin{bmatrix} T_1 \\ T_2 \\ T_3 \\ T_4 \\ T_5 \\ T_6 \end{bmatrix} \quad (17)$$

Thus, the final dynamic transfer matrix from end-effector to base is:

$$\tau = \begin{bmatrix} e_{M_1} & \cdots & e_{M_6} \\ e_{l_1} & \cdots & e_{l_6} \end{bmatrix} \begin{bmatrix} \frac{\vec{e}_{l_1}.\vec{e}_{N_1}}{|\vec{a}_1|} & \cdots & 0 \\ \vdots & \ddots & \vdots \\ 0 & \cdots & \frac{\vec{e}_{l_6}.\vec{e}_{N_6}}{|\vec{a}_6|} \end{bmatrix} \quad (18)$$

τ is a matric that defines the equation of motion base on states on end effector and torques on rotary motors, which leads us to implement torque control directly.

C. *Dynamic equation evaluation and driving nonlinear Model*

As we have some simplified assumptions to derive the dynamic equations, having a valid non-linear system is necessary to evaluate the controllers design accordingly.

As some constraints could not be considered in MATLAB software (e.g., collision, hardness and elasticity of bodies, and friction), ADAMS software is utilized to simulate hexapod robot's dynamic model. The only problem with ADAMS software is insufficient infrastructure to implement some non-linear controllers directly. Thus, in order to control a non-linear system in ADAMS, the software is connected to MATLAB and controlled online.

Firstly, the system is designed in SolidWorks (Fig. 3) then the mentioned design is entered in ADAMS and the essential constraint such as joints constrains, mass and materials of members the bodies rigidity toward each other and friction are applied on it. The information about design assumption are presented in Table I.

As it shown in Table I, the system has 14 component of mass, and moment of inertias are present in the table.

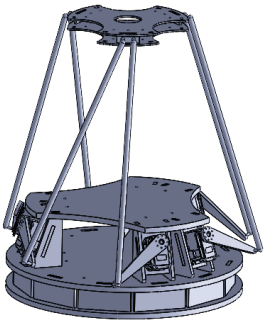

Fig. 3. Designed system in solidworks software

TABLE I. PARAMETERS USED IN ADAMS AND MATLAB SOFTWARE.

Qty.	Dimension(cm)	Inertia (kg.m^2)	Mass (kg)	Parts
6	40.4	I_x=0.0016 I_y=0.0016 I_z=0.000001	0.08	Links connected to end effector
6	11	I_x=0.000001 I_y=0.000058 I_z=0.000060	0.04	Links connected to motor
1	Circle(R=11)	I_x=0.003 I_y=0.003 I_z=0.006	1	End effector
1	Circle(R=20)	I_x=0.027 I_y=0.027 I_z=0.054	7	Base

As it specified in Fig. 4 the constraints are applied on the system. Also it is assumed a bidirectional torque on each leg that is shown with red color.

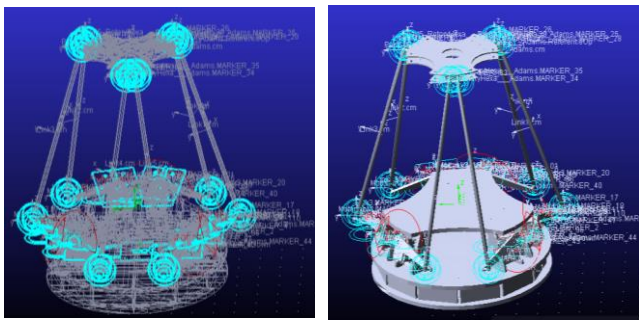

(a) (b)

Fig. 4. Designed system with constraints in ADAMS Software. (a) Lucid view. (b) Opaque view.

III. CONTROLLING HEXAPOD'S DYNAMICS

Namely, the designed dynamic system in the ADAMS software is noticeably nonlinear, and in order to control the system, a controller should be capable to reject the tracking errors, considering the non-linearity. Also, optimizing the inputs in parallel robots are always challenging. Therefore, an LQI optimal controller is designed and employed to control the system as follow.

A. *State-space equations:*

To design an optimal controller, it's prerequisite to find the state space of the dynamic model. To this end, we can formulate the dynamic equations as follow.

$$\dot{\bar{x}} = \bar{A}\bar{x}(t) + \bar{B}(t)T(t) + \bar{d}(t) \tag{19}$$

Consequently, dynamic of error is introduced as

$$\dot{\bar{e}}(t) = \bar{A}\bar{e}(t) + \bar{B}(t)T(t) + \bar{d}(t) \tag{20}$$

Where Matrix T consists of manipulated torques, and $\bar{d}$ is time variant disturbance. e is error matrix of the states and described as $\bar{e} = \bar{x} - x_d$, where x_d includes desire values of each states. Matrix $\bar{A}$, composed of elements $a_{i,j}$ in (21), reflects the dynamic of the system. Finally, matrix $\bar{B}$, composed of elements $b_{i,j}$ in (22), reflects the interconnections among the manipulated torques and corresponded state. The matrices for the mentioned system can be described as:

$$a_{i,j} = \begin{cases} 0 & if\ i = 2k \\ 1 & if\ i = 2k-1, and\ j = i+1 \\ 0 & otherwise \end{cases} \tag{21}$$

$$b_{i,j} = \begin{cases} \tau\left(\frac{i}{2}, j\right) & if\ i = 2k \\ 0 & otherwise \end{cases} \tag{22}$$

Where $k = 1, \dots, 6$. In presence of disturbances (e.g., Uncertainty in dynamic parameters), we employ an integral controller to reject constant disturbances [26]. Thus, we formulate our problem by augmenting the original system (20) with S (i.e., as many as number of links) integral states, where,

$$\dot{z}(t) = \bar{C}\bar{e}(t) \tag{23}$$

where C consists of $\bar{c}_{i,j}$ denoted as follow.

$$\bar{c}_{i,j} = \begin{cases} 1 & if\ j = 2i-1, and\ i = k \\ 0 & otherwise \end{cases} \tag{24}$$

The resulting augmented system reads:

$$\dot{e}(t) = Ae(t) + B(t)T(t) + d(t), \tag{25}$$

where,

$$e = \begin{bmatrix} \bar{e} \\ z \end{bmatrix},\ d = \begin{bmatrix} \bar{d} \\ - - - - - \\ 0_{S\times(2S)} \end{bmatrix},$$

$$A = \begin{bmatrix} \bar{A} & | & 0_{H\times S} \\ - - - & - & - - - \\ \bar{C} & | & 0_{H\times S} \end{bmatrix}, B = \begin{bmatrix} \bar{B} \\ - - - - - \\ 0_{S\times(F+1)} \end{bmatrix}, C = [\bar{C} \quad I_{H\times S}].$$

Finally, we define the following quadratic cost function, over an infinite time horizon, which accounts for minimization of all states and control inputs:

$$\min J = \sum_{k=0}^{\infty}[e^T(t)Qe(t) + u^T(k)Ru(k)] \tag{26}$$

where,

$$Q = \omega_Q I_{3S\times 3S},\ R = \omega_R I_{S\times S}. \tag{27}$$

Matrices Q and R are weighting matrices associated to the magnitude of all states and control actions, respectively, defined by parameters $\omega_Q > 0$, and $\omega_R > 0$.

The resulting optimal control problem (23), (22) can be solved through a Linear Quadratic Regulator (LQR), which provides a stabilizing feedback gain under the assumptions that the original system is, at least, stabilisable and detectable (see chapter 2 of [27])

B. Stability and detectability:

We investigate stabilisability and detectability of system (25) by employing the Hautus-test [28]. According to [28], to guarantee that the pair (A, B) is stabilisable, B must have more linearly independent columns than the number of non-stable $(\lambda \leq 0)$ modes. Depending on the system topology, matrix A has zero columns equal to number of links, which is cancelled with columns of B and satisfies stabilisability criteria as:

$$rank\,[(\lambda I - A) \quad B] = 3S. \tag{28}$$

We turn now our attention to the detectability of the pair (A, C^TQC); according to [29], since $Q > 0$ this is equivalent to investigating the detectability of the pair (A, C). In our case, the Hautus test condition as follow, is verified in case C has at least a non-zero element in each column corresponding to a marginally stable mode ($\lambda = 0$). Note that, in all the described cases, the system is also observable.

$$rank\begin{bmatrix} \lambda I - A \\ C \end{bmatrix} = 3S. \tag{29}$$

C. Controller design:

The solution to the proposed LQI problem is the linear feedback control law.

$$u(t) = Ke(t), \tag{30}$$

where,

$$K = (R + B^TPB)^{-1}B^TPA, \tag{31}$$

$$P = C^TQC + A^TPA - A^TPB(R + B^TPB)^{-1} \tag{32}$$

The optimal gain (31) and the Algebraic Riccati Equation (32) can be found in classic Optimal Control books (see, e.g., [30]). For practical implementation, the gain K is appropriately split as:

$$K = [K_p \quad | \quad K_I], \tag{33}$$

which allows to rewrite the control law as:

$$u(t) = -K_P\bar{e}(t) - K_I z(t) \tag{34}$$

The feedback control law (34) is very effective for practical application since the computation of the feedback gains K_P, K_I for the mention system needs less effort.

D. ANFIS estimator design for ω_Q, and ω_R

As the parameters of dynamic equation in (22) are time variants, thus $\bar{B}(t)$ is time variant respectively, which concludes to have nonlinear error dynamic in (20). Accordingly, the system is supposed to have different behaviour in different path. Then, the system and optimization method are non-linear and the complexity of the problem reveals the need of intelligent methods able to overcome the complexity and non-linearity. As the cost function of minimization problem in (26) is dependant to ω_Q, and ω_R finding a solution to estimate exact ω_Q, and ω_R in each time interval is a breakthrough to overcome the non-linearity. To this end, here a novel input-output model based on ANNs is presented to estimate ω_Q, and ω_R as real-time. The most important point in this approach is choosing proper inputs and outputs. Based on (26), ω_Q is weight of penalizing the states error, and ω_R minimizes designed torques. Thus, functions of the state errors and toques are appropriate candidates for estimator inputs.

The functions are chosen according to [31]. Accordingly, for our problem density function of state error and torques are suitable functions to describe the changes which is extracted as follow.

$$\rho_{\bar{e}}(t) = (m+1)\frac{\bar{e}(t)}{\sum_{i=n-m}^{n}\bar{e}(t(i))} \tag{35}$$

$$\rho_T(t) = (m+1)\frac{T(t)}{\sum_{i=n-m}^{n}T(t(i))} \tag{36}$$

Where, $\rho_{\bar{e}}$ is density of error of state and ρ_T is density of torques. To clarify, (35), and (36) are sensitive when $e(t)$ and $T(t)$ are considerably greater than average of the variables with window size $m+1$. These criterion defines a smooth and logical instigation to changes of the variable [31]. Accordingly, the inputs of the ANN estimator are $\rho_{\bar{e}_{1\times 6}}$, and $\rho_{T_{1\times 6}}$, and the outputs are $\omega_{Q_{1\times 1}}$, and $\omega_{R_{1\times 1}}$ as depicted in Fig. 5. To design an ANN estimator, a data-set of the inputs-outputs is needed, thus the controller of (34) used as master for the estimator. For collecting the data, we controlled the robot with different amounts of ω_Q, and ω_R as 0.1, 1, and 10, which includes 9 experiments. In each experiments range of end-effector angles' variation is between $\frac{\pi}{6}$, and $-\frac{\pi}{6}$ (rad), and transformation is 0.3 (m) in each three main direction of X, Y, and Z. Moreover, range of frequency varies from 1 to 5 Hz. Then the proper inputs-outputs of the estimator are prepared with sample number of 14400.

Addressing structure of ANN estimator, There is one hidden layer with ten nods, and the back-propagation algorithm is employed to train this estimator. Back propagation is a general-purpose network paradigm and calculates the errors between the desired and the actual output and propagates the error back to each node in the network. Thus, the back-propagated error drives the learning at each node [32].

In the development of the ANN estimator, the prepared data is usually divided into two randomly selected subsets.

Respectively, they are the training and testing data-set. First data-set is utilized to develop and calibrate the estimator. The second data subset, which is introduced as the validation data-set and not used in the development of the estimator, is used to validate the performance of the trained estimator. Accordingly, 70% of the master data-set is employed for training and testing purposes, and the remaining 30% is set aside for model validation.

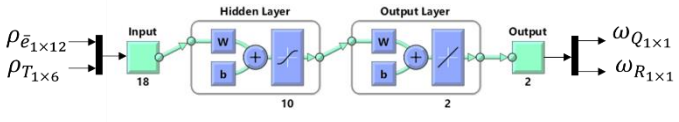

Fig. 5. Designed ANN estimator structure.

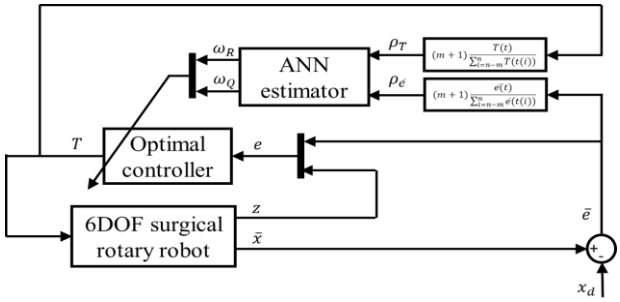

Fig. 6. Control diagram.

IV. EXPERIMENT RESULTS

According to above explanation, the robot's states and desired angles, and torques are shown in Fig. 5 simultaneously. In this figure, the desired amounts are inputted due to (30) and (31), and the other amount are assumed as zero. Also, ω_Q and ω_R, as controller parameters in (27), are considered as 1. The angles' values are considered as follow.

$$\emptyset(t) = \frac{\pi}{6} Sin(2t) \tag{37}$$

$$Z = 0.05Sin(2t) + 0.3 \tag{38}$$

Where t is time. Considering Fig. 5(b), the controller could reject the errors by the time. Actually, the integral states are around zero at second 5, thus the error reduces and the system is going to trace the target (sensor's data) with the minimum error. Also, torques on the system are shown in Fig. 5(b), which are useful for choosing electromotor and system designing for manufacturing regarding to reliable simulated dynamic of the robot in ADAMS software.

V. CONCLUSION

This paper presents a control methodology for a parallel robot introduced as a surgical robot, capable to simulate all angular motions and transition. Furthermore, kinematic, dynamic and control analysis are studied on the mechanism equations of direct/inverse kinematic of the parallel robot, derived and implemented in ADAMS software. In order to have a well desired amount tracking by end effector, the existing dynamic is controlled as online, using LQI controller in MATLAB software. Finally, the simulation results showed that the optimal LQI controller was able to control dynamic of the system and penalize the tracking error in presence of disturbance, which is one of integral controller properties. We are currently investigating sensitivity of controller parameters on stability of the system, as well as producing further simulation experiments to investigate robustness to parameter

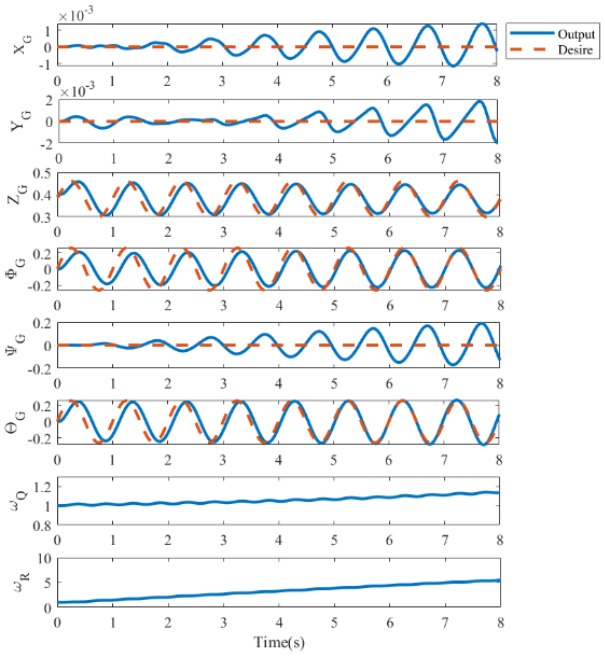

(a)

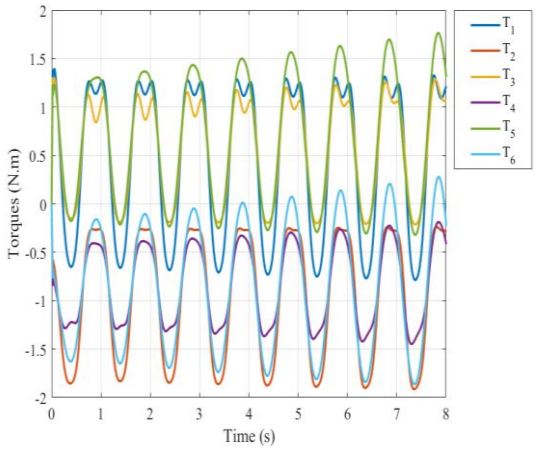

(b)

Fig. 7. Control performances. (a) Main states, and ANN estimator output. (b) Motor torques.

choices, which are going to be introduced in a future publication.

REFERENCES

[1] N. Y. Siddiqui, M. L. Galloway, E. J. Geller, I. C. Green, H.-C. Hur, K. Langston, M. C. Pitter, M. E. Tarr, and M. A. Martino, "Validity and reliability of the robotic objective structured assessment of technical skills", Obstetrics and gynecology, vol. 123, no. 6, p. 1193, 2014 (cit. on p. 1).

[2] E. Ritter and D. Scott, "Design of a Proficiency-based Skills Training Curriculum for the Fundamentals of Laparoscopic Surgery",Surgical Innovation, 2007 (cit. on p. 1).

[3] A. P. Stegemann, K. Ahmed, J. R. Syed, S. Rehman, K. Ghani, R. Autorino, M. Sharif, A. Rao, Y. Shi, G. E. Wilding,et al., "Fundamental skills of robotic surgery: A multi-institutional randomized controlled trial for validation of a simulationbased curriculum",Urology, 2013 (cit. on p. 1).

[4] B. F. Buxton and S. D. Galvin, "The history of arterial revascularization: From kolesov to tector and beyond",Annals of cardiothoracic surgery, vol. 2, no. 4, p. 419, 2013 (cit. on p. 1).

[5] G. Kunz and G. Leyendecker, "Uterine peristaltic activity during the menstrual cycle: Characterization, regulation, function and

dysfunction", Reproductive biomedicine online, vol. 4, pp. 5–9, 2002 (cit. on p. 1).

[6] D. Stewart, "A platform with six degrees of freedom", Proceedings of the institution of mechanical engineers, vol. 180, no. 1, pp. 371–386, 1965 (cit. on pp. 1, 2).

[7] V. E. Gough, "Contribution to discussion of papers on research in automobile stability, control and tyre performance, by cornell staff", inProceedings of the Automotive Division of the Institution of Mechanical Engineers, 1956, pp. 392–395 (cit. on pp. 1, 2).

[8] E.F. Fichter, A Stewart platform- based manipulator: general theory and practical construction, Int. J. Rob. Res. 5 (1986) 157–182, doi: 10.1177/027836498600500216 .

[9] J.-P. Merlet , Force-feedback control of parallel kinematics manipulators, Kinematic and Dynamic Issues in Sensor Based Control, Springer, 1990, pp. 143–158 .

[10] K. Sugimoto , Computational scheme for dynamic analysis of parallel manipulators, J. Mech. Trans. Autom. Des. 111 (1989) 29–33 .

[11] W.O.D. Do , D.C.I. Yang , Inverse dynamic analysis and simulation of a platform type of Roboir, J. Robot. Syst. 5 (1988) 209–227 .

[12] B. Dasgupta, T.S. Mruthyunjaya, A Newton–Euler formulation for the inverse dynamics of the Stewart platform manipulator, Mech. Mach. Theory 33 (1998) 1135–1152, doi: 10.1016/S0094- 114X(97)00118- 3.

[13] G. Lebret, K. Liu, Dynamic analysis and control of a Stewart platform manipulator, J. Robot. Syst. 10 (1993) 629–655. http://onlinelibrary.wiley.com/doi/10.1002/rob.4620100506/abstract.

[14] A.M. Lopes, Dynamic modeling of a Stewart platform using the generalized momentum approach, Commun. Nonlinear Sci. Numer. Simul. 14 (2009) 3389. http:// dx.doi.org/ 10.1016/ j.cnsns.2009.01.001 .

[15] L.-W. Tsai, Solving the inverse dynamics of a Stewart-Gough manipulator by the principle of virtual work, J. Mech. Des. 122 (2000) 3, doi: 10.1115/1.533540.

[16] J. Gallardo, J.M. Rico, A. Frisoli, D. Checcacci, M. Bergamasco, Dynamics of parallel manipulators by means of screw theory, Mech. Mach. Theory 38 (2003) 1113–1131, doi: 10.1016/S0094- 114X(03)00054- 5 .

[17] Q. Meng, T. Zhang, J. He, J. Song, J. Han, Dynamic modeling of a 6-degree-of-freedom Stewart platform driven by a permanent magnet synchronous motor, J. Zhejiang Univ. Sci. C 11 (2010) 751–761, doi: 10.1631/ jzus.C0910714.

[18] M. Liu , C. Li , C. Li , Dynamics analysis of the Gough–Stewart platform manipulator, IEEE Trans. Robot. Autom. 16 (2000) 94–98 .

[19] S. Staicu, D. Zhang, A novel dynamic modelling approach for parallel mechanisms analysis, Robot, Comput. Integr. Manuf. 24 (2008) 167–172, doi: 10.1016/j.rcim.2006.09.001 .

[20] B.R. Hopkins, R.L. Williams, Kinematics, design and control of the 6-PSU platform, Ind. Robot Int. J. Robot. Res. Appl. 29 (2002) 443–451, doi: 10.1108/01439910210440264.

[21] S.-H. Lee, J.-B. Song, W.-C. Choi, D. Hong, Position control of a Stewart platform using inverse dynamics control with approximate dynamics, Mechatronics 13 (2003) 605–619, doi: 10.1016/S0957-4158(02)00033- 8 .

[22] E. Akdoğan, M. E. Aktan, A. T. Koru, M. S. Arslan, M. Atlıhan, & B. Kuran. "Hybrid impedance control of a robot manipulator for wrist and forearm rehabilitation: Performance analysis and clinical results". Mechatronics, 49, 77-91, 2018.

[23] H. Navvabi, & A. H. Markazi."Hybrid position/force control of Stewart Manipulator using Extended Adaptive Fuzzy Sliding Mode Controller (E-AFSMC)". ISA transactions, 88, 280-295, 2019.

[24] H. Navvabi,& A. H. D. Markazi. "New AFSMC method for nonlinear system with state-dependent uncertainty: Application to hexapod robot position control". Journal of Intelligent & Robotic Systems, 95(1), 61-75, 2019.

[25] X. Yang, H., Wu, B., Chen, S., Kang, & S. Cheng. " Dynamic modeling and decoupled control of a flexible Stewart platform for vibration isolation". Journal of Sound and Vibration, 439, 398-412, 2019.

[26] K. J. Astrom and T. Hagglund, PID controllers: theory, design, and tuning, 1995

[27] F. L. Lewis, D. L. Vrabie, and V. L. Syrmos, Optimal Control. John Wiley & Sons, Inc., 2012.

[28] B R. L. Williams and D. A. Lawrence, Linear state-space control systems. Hoboken, NJ, USA: John Wiley & Sons, Inc., 2007.

[29] B. D. O. Anderson and J. B. Moore, Linear optimal control. Prentice-Hall, 1971.

[30] J. P. Hespanha, "Linear systems theory. 2009." ISBN-13: 978-0.

[31] B. Tarvirdizadeh, A. Golgouneh, F. Tajdari, and E. Khodabakhshi. "A novel online method for identifying motion artifact and photoplethysmography signal reconstruction using artificial neural networks and adaptive neuro-fuzzy inference system," Neural Computing & Applications: 1-18, 2018.

[32] B. Kosko, Neural Networks and Fuzzy Systems. Upper Saddle River, NJ: Prentice-Hall, 1991.